Remote Sensing of Aerosol Properties Using NOAA AVHRR Data over the Northeastern Asian Seas: Development of Retrieval System

Hironobu IWABUCHI*, Akira SOBAJIMA**,

Jun-ichi KUDOH*, Shoji ASANO**

Keywords: aerosol, remote sensing, AVHRR, environment

Abstract

A retrieval system to infer properties of aerosol particles from AVHRR multi-spectral measurement was developed with an objective to detect a decadal-scale variation in aerosol properties and spatial distribution in the northeastern Asian region. The algorithm was based on theoretical radiative transfer simulation and optimized for accurate retrieval of aerosol properties over the northeastern Asian seas. Error analyses showed that our algorithm is accurate enough to study seasonal and regional variation of aerosol property. We utilized the advantage of 1-km resolution for precise cloud screening. It was demonstrated that various kinds of cloud including thin broken cloud are appropriately excluded from the retrieval with our cloud screening procedure using multi-spectral and textual characterization. A first result showed an interesting phenomenon of transport of mineral dust aerosol from the continent to Japan.

1. Introduction

One of the key issues in the climate research is to evaluate the impact of aerosol induced from human activity. The optical properties of aerosol particles determine a governing impact on future climate change of the earth. Chemical composition, particle size and its solar radiative effect of aerosol particles varies largely by its source; water soluble particle such as sulfate emitted from industrial activity, mineral dust aerosol such as seen in "Kosa" event, sea salt particle generated by wind stress on sea surface, and soot particle emitted from biomass burning and industrial activity. The Advanced Very High Resolution Radiometer (AVHRR) data have been used to retrieve global aerosol distribution, based on one-or two-channel algorithm (Husar et al., 1997; Stowe et al., 1997; Higurashi and Nakajima, 1999; Higurashi et al., 2001).

We developed a retrieval system to infer properties of aerosol polydispersion using AVHRR multi-spectral measurement from space. An objective in the present study is to detect a decadal-scale variation in aerosol properties and spatial distribution in the

* Center for Northeast Asian Studies, Tohoku University

** Center for Atmospheric and Oceanic Studies, Graduate School of Science, Tohoku University

northeastern Asian region. The algorithm was optimized for aerosol research over the northeastern Asian seas. Our algorithm utilizes the advantage of 1 km resolution for precise cloud screening instead of 4 km resolution in the previous studies (Husar et al., 1997; Stowe et al., 1997; Higurashi and Nakajima, 1999; Higurashi et al., 2001). In this report, the algorithm and procedure are described, and a first result is presented.

2. Data

The satellite data used in the present work are obtained with AVHRR aboard NOAA polar orbiter satellite. NOAA polar orbiter satellites fly in sun-synchronous orbit with a nominal inclination angle of 100° and nodal period of about 100 minutes (Kidwell, 1991). The data from afternoon orbit of NOAA-11 and -14 spacecrafts are used. The local solar time of passing of the spacecraft is 12:30−16:00 (Kidwell, 1991). AVHHR is a scanning sensor with a nominal spatial resolution of 1.1 km at nadir and has five spectral bands: channels 1 (0.58−0.68 μm), 2 (0.725−1.10 μm), 3 (3.55−3.93 μm), 4 (10.3−11.3 μm), and 5 (11.5−12.5 μm). The AVHRR data used here were processed from High Resolution Picture Transmission (HRPT) data, which have been collected in Sendai, Japan since 1980s (Kawamura et al., 1993a). A HRPT data image requires a geometrical correction since it is distorted by surface curvature and rotation of the earth. The data were sampled in 1.1-km nominal spatial resolution with the geometrical correction, by nearest-neighbor interpolation. For infrared channels (channels 3, 4 and 5), nonlinear radiometric correction was applied (Kawamura et al., 1993b). It is well known that the gains of AVHRR solar bands (channels 1 and 2) degrade during the lifetime of spacecraft in its orbit. We have applied the sensor calibration for the two channels following formulas in Iwabuchi (2001). The spectral radiance for ith channel (i = 1, 2), I_i (W m^{-2} sr^{-1} μm^{-1}), was converted to the bi-directional reflection function, R_i (%), by the following formula:

$$R_i = (\delta_0)^2 \frac{\pi I_i}{\mu_0 F_{0i}},$$

where δ_0 denotes the sun-earth distance normalized to annual mean (in astronomical unit), μ_0 cosine of solar zenith angle, and F_{0i} the annual mean extraterrestrial solar irradiance (Wm^{-2} μm^{-1}). The term of $(\delta_0)^2$ is for a correction for varying distance between the sun and the earth.

The target region for the analysis is the northwestern Pacific Ocean and the seas of Japan, Okhotsk, and East China. The region is divided into fourteen sub-regions (Fig. 1). Climatic data of precipitable water for clear-sky area, wind velocity at surface and column-integrated ozone content are prescribed for each sub-region and month. These data are provided from database of da Silva et al. (1994) and the NCEP/NCAR reanalysis (Kalnay et al., 1996).

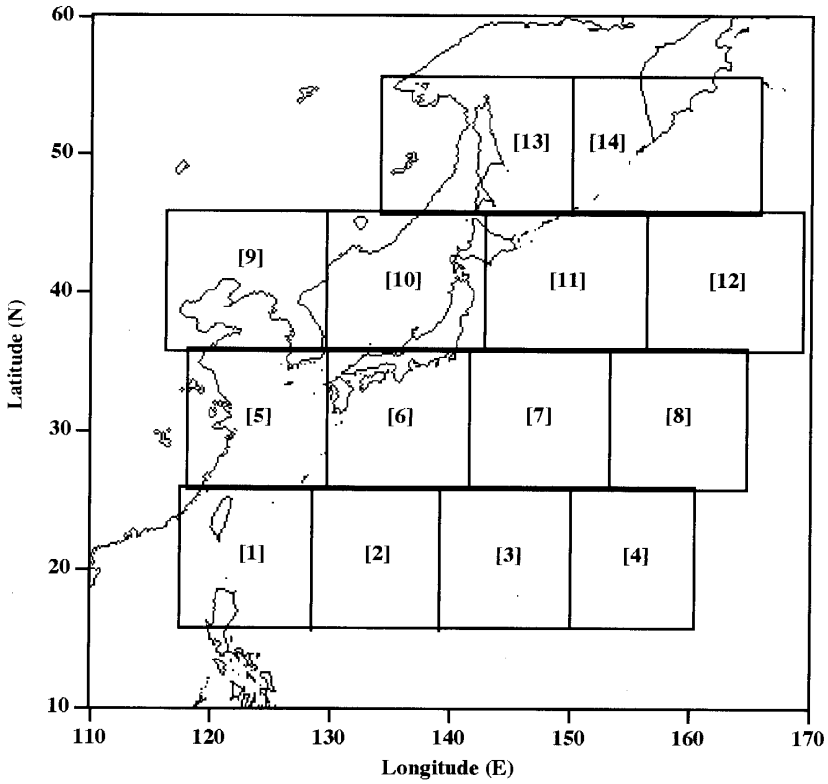

Fig. 1. Geographical locations of target sub-regions.

3. Algorithm

In the following, we describe an algorithm to infer aerosol optical thickness and Ångström exponent from AVHRR data over seas. The Ångström exponent (α) is a measure of power-law dependency of spectral optical thickness on wavelength and defined by $\tau(\lambda) = \beta\lambda^{-\alpha}$, where λ denotes the spectral wavelength and β a coefficient. First, look-up-table (LUT) of theoretical reflection functions of channels 1 and 2 are prepared before the data analysis. After cloud screening, the aerosol optical thickness and Ångström exponent is derived for clear-sky pixel, from comparison of observed AVHRR data with the LUT.

3.1. Look-up-table

Look-up-tables were prepared by theoretical radiative transfer calculation with a code of Nakajima and Tanaka (1986, 1988), in which the discrete ordinate and adding methods were used and gaseous absorption was incorporated by using k-distribution with LOWTRAN-7 (Kineizys et al., 1988). A rough ocean model of Nakajima and Tanaka (1983) was also used, so that effect of wind velocity on the roughness of ocean surface was modeled. The spectral radiance was calculated from integration weighted by filter response function over 27 spectral bands for channel 1 and 43 bands for channel 2. A model atmosphere was divided into seven layers; the boundaries are at 0 km, 1 km, 2 km, 3 km, 4 km, 7 km, 12 km, and 120 km. The gaseous constituents such as oxygen were referred to the U.S. Standard Atmosphere (Kneizys et al., 1988). Following Higurashi and Nakajima

(1999), the absorption by ozone was corrected as

$$R = R' \exp[-\tau_{O3}(1/\mu + 1/\mu_0)],$$

where R and R' denotes reflection function calculated with and without ozone absorption, τ_{O3} the optical thickness of ozone, μ the cosine of the viewing zenith angle.

It is assumed that the aerosol particles distribute at altitude of 0−3 km and that the density is constant. The volume size distribution was assumed bimodal and lognormal,

$$\frac{dV}{d\ln r} = \sum_{n=1}^{2} C_n \exp\left[-\frac{1}{2}\left\{\frac{\ln(r/r_{mn})}{\ln s_n}\right\}^2\right]$$

where V denotes volume of aerosol particles, r radius of the particle, C_n coefficient determining first $(n = 1)$ and second $(n = 2)$ distribution peak value, r_{mn} mode radius, s_n standard deviation. According to review of previous ground-based measurements in Higurashi and Nakajima (1999), we assumed $r_{m1} = 0.17\,\mu$m, $r_{m2} = 3.4\,\mu$m, $s_1 = 2.0$, and $s_2 = 3.4$. The complex refractive index of aerosol particle was assumed as $m = 1.5 - 0.005i$. The single scattering properties of aerosol particles were calculated by Mie-theory, assuming spherical particle. When the mode radii and widths of bimodal distribution are given a priori, the Ångström exponent shows one-to-one relation with the peak ratio, C_1/C_2. The Ångström exponent is a measure of mean size of aerosol particles; small a is associated with large mean size and vice versa. In the present study, we calculated a by fitting power-law function to spectral optical thickness at eleven wavelengths of 0.6−1.0 μm with a spacing of 0.05 μm.

The look-up-table was made for the aerosol optical thickness, Ångström exponent, solar and viewing zenith angles (θ_0 and θ, respectively), relative azimuth angle (ϕ), wind velocity, and precipitable water. The grid system of these parameters is summarized in Table 1. The theoretical reflection function is interpolated from the look-up-table for an angular geometry of observation. The two-channel reflection functions for various t and a are shown in Fig. 2. Note that here and hereafter, the aerosol optical thickness is for a spectral

Table 1. Grid system for the look-up-table of AVHRR channel 1 and 2 theoretical reflection functions: aerosol optical thickness, τ, Ångström exponent, α; solar zenith angle, θ_0; viewing zenith angle, θ; relative azimuth angle, ϕ.

Parameter	Grid values [Min-Max (spacing)]	Number of grids
τ	0.03, [0.1−1.5 (0.1)]	16
α	−0.1, 0, 0.2, 0.4, 0.65, 0.9, 1.2, 1.5, 1.8	9
$\cos\theta_0$	[0.34−1 (0.03)]	23
$\cos\theta_0$	[0.7−1 (0.02)]	16
ϕ (°)	[0−180 (10)]	19
Precipitable water (g cm^{-1})	[0−5 (0.5)]	11
Wind velocity (m s^{-1})	[5−12 (1)]	8

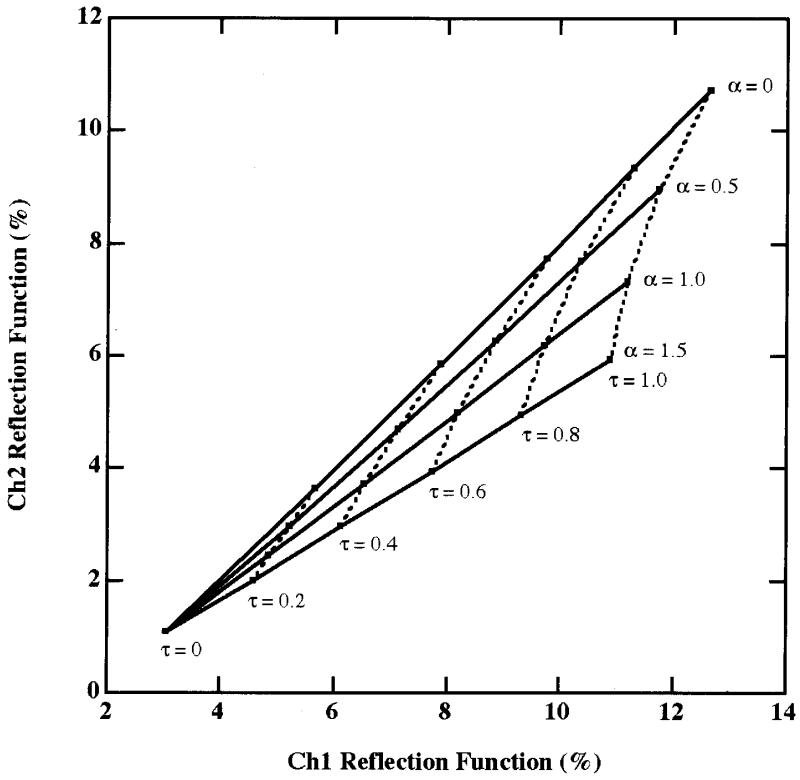

Fig. 2. Theoretical relationship of AVHRR channels 1 and 2 reflection function with aerosol optical thickness (τ) and Ångström exponent (α); $\theta_0 = 30^\circ$, $\theta = 40^\circ$, $\phi = 180^\circ$.

wavelength of 0.5 μm. Reflectance of channel 2 is large for small α, i.e. for large size of particle. If a pair of observed two-channel reflection function is given, τ and α can be determined by interpolation from the array of theoretical reflection function.

The retrieval is done only for $\theta_0 < 70^\circ$ and $\theta < 45^\circ$. The sun glint geometry is identified by the cone angle (Θ_c), which is defined as an angle between target-to-satellite direction and mirroring direction of target-to-sun one, i.e.,

$$\cos\Theta_c = \mu\mu_0 - \sqrt{1-\mu^2}\sqrt{1-\mu_0^2}\cos\phi,$$

where $\mu = \cos\phi$. Single solution of the pair of τ and α could not be obtained for small Θ_c since the ocean surface is highly reflective. In addition, the reflection function for small Θ_c highly depends on wind velocity at the surface. The data for $\Theta_c < 45^\circ$ are avoided from the retrieval. Data over land are excluded from retrieval analysis since with our algorithm remote sensing of optically thin aerosol polydispersion is impossible over land surface with high reflectivity.

3.2. Error analysis

A main uncertainty of retrieved Ångström exponent comes from varying precipitable water (Fig. 3) and vertical distribution of water vapor and also aerosol (Ignatov et al., 1998). The uncertainty by varying precipitable water is large for small α and dry

atmosphere. The maximum error in retrieved α is about 0.15 for perturbation of 0.5 g m^{-2} to 1.0 g m^{-2} in precipitable water. This error is almost the same as for change in altitude of aerosol layer from 0−3 km to 0−1 km when precipitable water is 2 g m^{-2} (Fig. 4). The aerosol optical thickness becomes slightly uncertain by varying wind velocity when cloud optical thickness is small, the wind velocity is large, and the cone angle is small. The maximum error in retrieved τ was estimated at 0.01 for τ = 0.1 and Θ_c = 60° when the wind velocity was changed by ± 3 m s^{-1} from 7 m s^{-1}. These errors are not significant to study seasonal and regional variation of aerosol property. The both retrieved quantities are sensitive to the mode radii (r_{m1} and r_{m2}) and the widths of size distributions (s_1 and s_2) (Higurashi et al., 2000) and also to imaginary part of refractive index (Fig. 5). However, our assumptions on the widths of size distributions and the refractive index are based on previous ground-based observations (Higurashi and Nakajima, 1999) and would be optimal to study statistical variation. In addition, retrieved quantities are meaningful as "equivalent" estimates with assumptions described in the previous subsection.

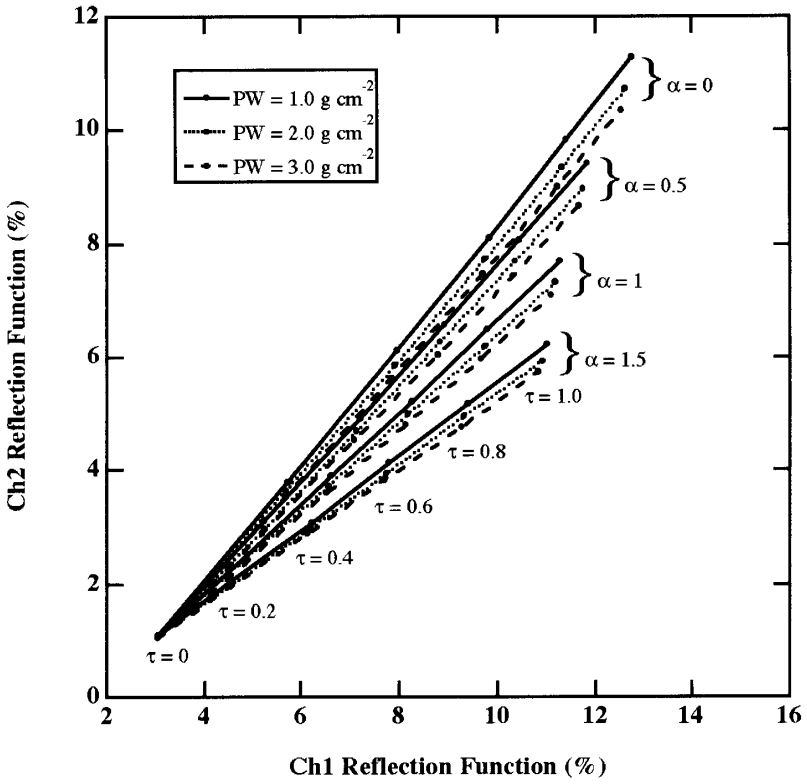

Fig. 3. Theoretical relationship of AVHRR channels 1 and 2 reflection function with aerosol optical thickness (τ) and Ångström exponent (α) for varying precipitable water (PW); θ_0 = 30°, ϕ = 40°, ϕ = 180°.

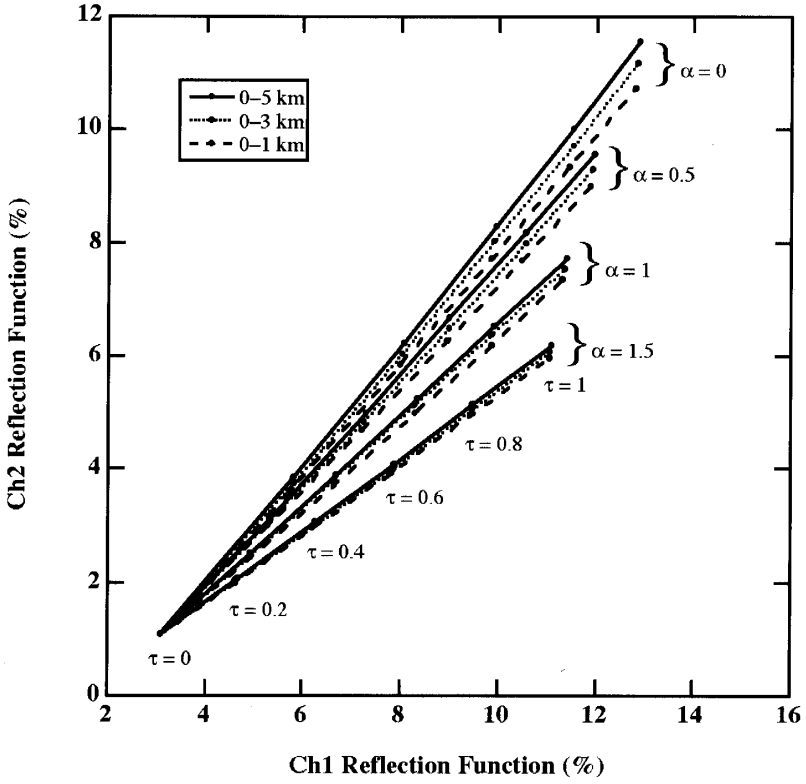

Fig. 4. As Fig. 3, except for varying altitude of aerosol layer.

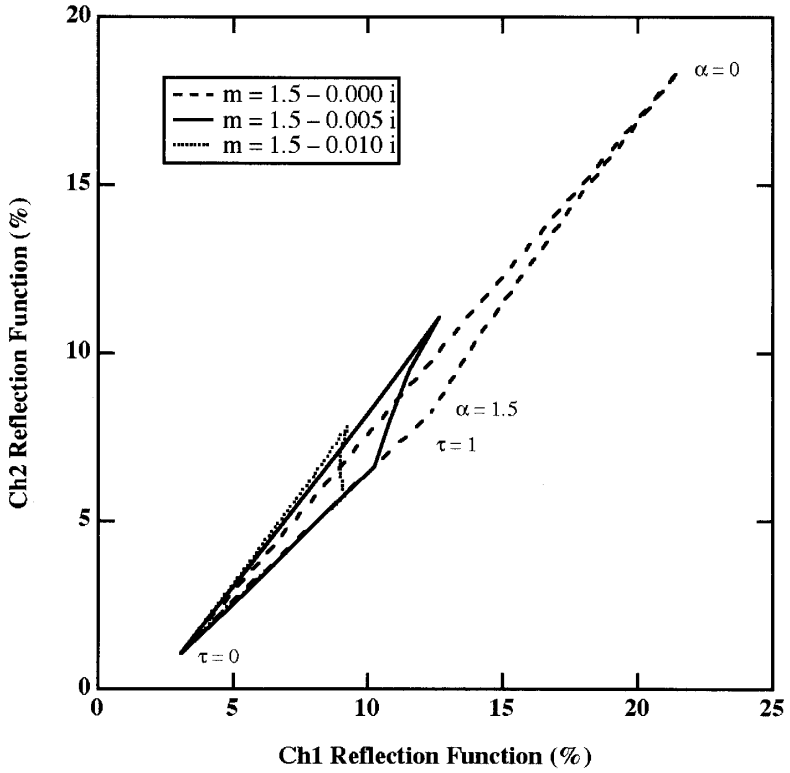

Fig. 5. Change of the array of theoretical reflection function by refractive index (m) of aerosol particle; $\theta_0 = 30^\circ$, $\theta = 40^\circ$, $\phi = 180^\circ$.

3.3. Cloud screening

Cloudy-sky pixels and their neighboring pixels are excluded from retrieval analysis. For that purpose we utilized an advantage of multi-spectral AVHRR data with spatial resolution of 1 km. The screening procedure is as follows:

1) Cold cloud pixels were detected by low brightness temperature in channel 4 (< 270K).
2) To avoid an optically thin cirrus cloud, we used a difference in the brightness temperature between the split window bands (channels 4 and 5). Cirrus cloud pixels were detected with the temperature difference larger than 2.5 K. Pixels of edge of broken cloud are also detected by this process.
3) Pixels with larger temperature difference between channels 3 and 4 than 5 K are identified as covered by water-phase bright cloud since in channel 3 signal solar reflection by water cloud is involved in addition to emission from surface and atmosphere.
4) Bright pixels with larger reflection function than theoretical value for $\tau = 1.5$ are identified as covered by water-phase thin cloud.
5) To avoid optically thin and broken cloud, 4×4-pixel grids with variance of channel 1 reflection function larger than 1.0% (in absolute unit) are excluded.
6) To avoid optically thin and isolated cloud, pixels with larger deviation than 1.0% (in absolute unit) in channel 1 reflection function from the 4×4-pixel mean are excluded.
7) To avoid three-dimensional radiative effect near cloud, 4×4-pixel grids with clear-sky coverage smaller than 50% are avoided. For the same purpose, pixels near the cloudy-sky pixel with a distance less than $1.1 \times [1 + 6(1 - \mu_0)]$ are excluded. This process is important to avoid unreal retrieval of very small optical thickness for cloud shadow pixel (Iwabuchi, 2001).

The remaining pixels are identified as clear-sky pixels without three-dimensional radiave effect, for these pixels the aerosol optical thickness and Ångström exponent are retrieved. The thresholds in the above seven processes were determined and optimized from theoretical radiative transfer simulation and extensive try-and-error tests.

4. A first result

A first result of the retrieval analysis is presented in Figs. 6 and 7. These are for a case of January 9, 1991 over the Japan Sea. Wind blew to southeast from the Siberian high in the northwest. The use of multi-spectral data is successful to detect various kind of cloud (Fig. 6). Clouds appear in the right bottom of the scene. At the beginning of generation of cloud, clouds are optically thin and broken. To detect these clouds is difficult with a threshold in brightness solely. Nevertheless, such clouds are appropriately excluded from the retrieval with our cloud screening procedure using textual characterization (Fig. 7). In the center of the scene, a thick aerosol band (with large τ) is found and it is associated with large particle size (small α). This could be considered as a flow of mineral dust aerosol from the continent. Along wind direction, the increase of optical thickness with decrease in Ångström exponent is shown. This suggests a growth in mean size of aerosol particles. A possibility is that the size increases for mineral dust particle coated by water soluble aerosol with supplying water vapor from the sea. Or the mean size may increase by addition of sea salt

particle generated by wind stress on the sea surface.

5. Conclusion

A retrieval system to infer properties of aerosol optical thickness and Ångström exponent from AVHRR multi-spectral measurement was developed. The algorithm was optimized for accurate retrieval of aerosol properties over the northeastern Asian seas and utilizes the advantage of 1-km resolution for precise cloud screening instead of 4-km resolution in the previous studies. Error analyses showed that our algorithm is accurate enough to study seasonal and regional variation of aerosol property. It was demonstrated that various kinds of cloud including thin broken cloud are appropriately excluded from the retrieval with our cloud screening procedure using spectral and textual characterization. Cloud neighboring pixels are also excluded to avoid the three-dimensional radiative effect such as cloud shadow. A first result showed an interesting phenomenon of transport of mineral dust aerosol from the continent to Japan. We are starting a twelve-year analysis with a goal to detect a decadal-scale variation in aerosol properties and spatial distribution in the northeastern Asian region.

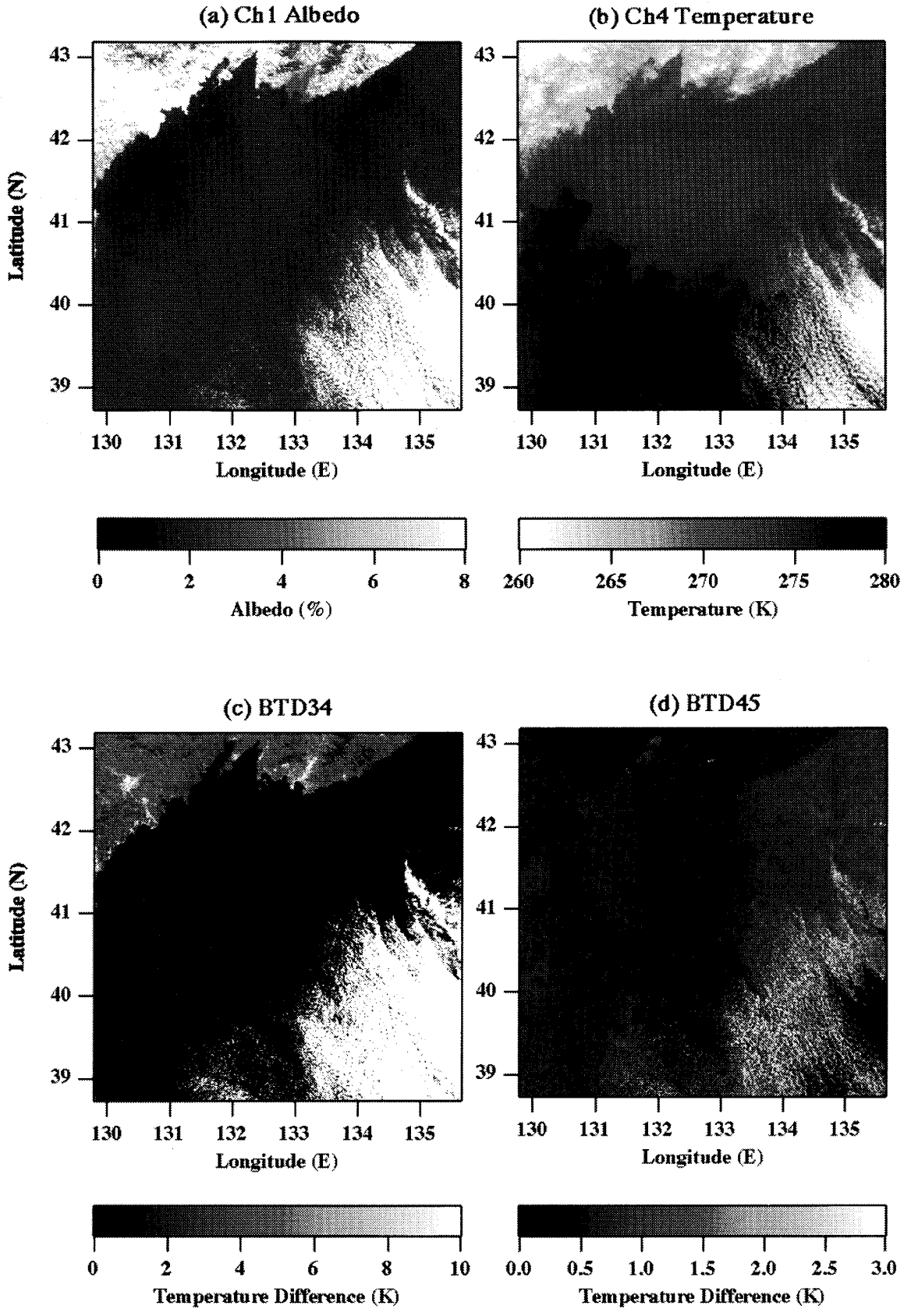

Fig. 6. Multi-spectral AVHRR images for the case of January 9, 1991: BTD34, brightness temperature difference between channels 3 and 4; BTD45, between 4 and 5.

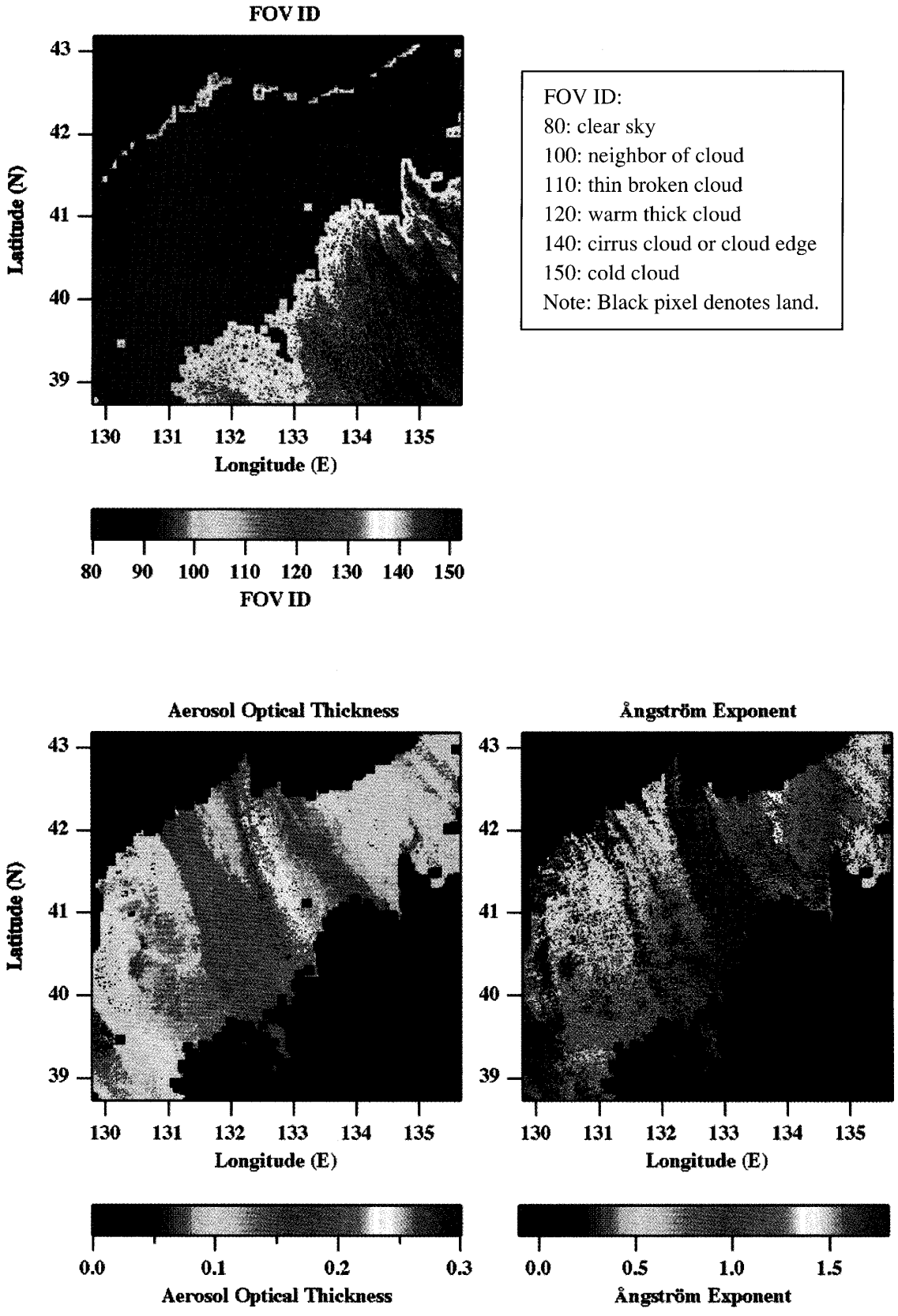

Fig. 7. Retrieval results of aerosol properties for the case of January 9, 1991. FOV ID denotes pixel classification result as explained in the upper right.

Acknowledgements

The authors are grateful to Prof. Kawamura of Center for Atmospheric and Oceanic Studies, Tohoku University for providing NOAA AVHRR data and a reviewer for helpful comments.

References

Higurashi, A., T. Nakajima, 1999: "Development of a two-channel aerosol retrieval algorithm on a global scale using NOAA AVHRR." *Journal of the Atmospheric Sciences,* **56**, 924－941.

Higurashi, A., Nakajima, T., Holben, B. N., Smirnov, A., Frouin, R., and Chatenet, B., 2000, "A study of global aerosol optical climatology with two-channel AVHRR remote sensing." *Journal of Climate,* **13**, 2011－2027.

Husar, R. B., J. M. Prospero, and L. L. Stowe, 1997: "Characterization of tropospheric aerosols over the oceans with the NOAA advanced very high resolution radiometer optical thickness operational product." *Journal of Geophysical Research,* **102**, 16889－16909.

Ignatov, A., L. Stowe, and R. Slingh, 1998: "Sensitivity of the Ångström exponent derived from AVHRR over the oceans." *Advanced Space Research,* **21**, 439－442.

Iwabuchi, 2001: "Calibration of the visible and near-infrared channels of NOAA-11 and -14 AVHRRs by reflections from molecular atmosphere and stratus cloud." *Submitted to International Journal of Remote Sensing.*

Kalnay, E., M. Kanamitsu, R. Kistler, W. Collins, D. Deaven, L. Gandin, M. Iredell, S. Saha, G. White, J. Woollen, Y. Zhu, M. Chelliah, W. Ebisuzaki, W. Higgins, J. Janowiak, K. C. Mo, C. Ropelewski, J. Wang, A. Leetmaa, R. Reynolds, Roy Jenne, and DennisJosheph, 1996: "The NCEP/NCAR 40-year reanalysis project." *Bulletin of the American Meteorological Society,* **77**, 437－471.

Kawamura, H., S. Kizu, F. Sakaida, and Y. Toba, 1993a: "The NOAA-HRPT data receiving system in the Center for Atmospheric and Oceanic Studies in the Tohoku University." *Tohoku Geophysical Journal (Science Report of Tohoku University, Series 5),* **34**, 89－102.

Kawamura, H., F. Sakaida, and S. Kizu, 1993b: "The AVHRR data processing system in the Center for Atmospheric and Oceanic Studies in the Tohoku University." *Tohoku Geophysical Journal (Science Report of Tohoku University, Series 5),* **34**, 103－114.

Kidwell, K. B., 1991: "NOAA Polar Orbiter Data User's Guide (*TIROS-N, NOAA-6, NOAA-7, NOAA-8, NOAA-9, NOAA-10, NOAA-11,* and *NOAA-12*)." NOAA Tech. Note, pp. 1-294 (Available from NOAA/NESDIS/National Climatic Data Center, Satellite Data Services Division, Princeton Executive Square, Room 100, Washington, DC 20233).

Kneizys, F. X., E. P. Shettle, L. W. Abreu, J. H. Chetwynd, G. P. Anderson, W. O. Gallery, J. E. A. Selby, and S. A. Clough, 1988: "Users Guide to LOWTRAN 7." *Rep. AFGL-TR-88-0177,* pp. 1－137.

Nakajima, T., and M. Tanaka, 1983: "Effect of wind-generated waves on the transfer of solar radiation in the atmosphere-ocean system." *Journal of Quantitative Spectroscopy and Radiative Transfer,* **29**, 521－537.

Nakajima, T., and M. Tanaka, 1986: "Matrix formulations for the transfer of solar radiation in a plane-parallel scattering atmosphere." *Journal of Quantitative Spectroscopy and Radiative Transfer,* **35**, 13－21.

Nakajima, T., and M. Tanaka, 1988: "Algorithms for radiative intensity calculations in moderately thick atmospheres using a truncation approximation." *Journal of Quantitative Spectroscopy and Radiative Transfer,* **40**, 51－69.

da Silva, A., A. C. Young, and S. Levitus, 1994: "Atlas of surface marine data 1994, Volume 1: Algorithms and procedures." *NOAA Atlas NESDIS,* **6**, U.S. Department of Commerce, Washington, D.C.

Stowe, L. L., and A. M. Ignatow, 1997: "Development, validation, and potential enhancements to the second-generation operational aerosol product at the National Environmental Satellite, Data, and Information Service of the National Oceanic and Atmospheric Administration." *Journal of Geophysical Research,* **102**, 16923－16934.